Status of simulations for EIC hadron polarimetry

Ana Sofia Nunes (BNL)

April 1, 2020

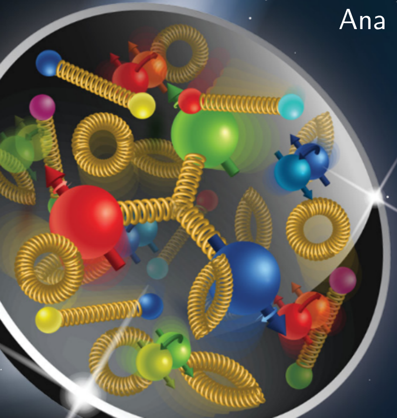

BROOKHAVEN NATIONAL LABORATORY
U.S. DEPARTMENT OF ENERGY | Office of Science

Simulation of current RHIC H-Jet polarimeter

Generated events: 1M, $E_{\mathrm{beam}} = 255$ GeV, w/ detector acceptance cut

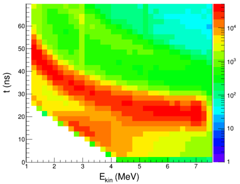

2017 Hjet data

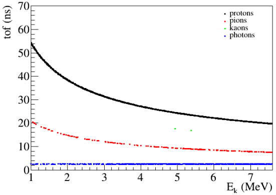

Pythia6 pp simulation
non elastic events, $\sigma_t = 0$

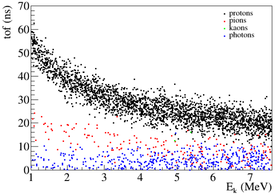

Pythia6 pp simulation
non elastic events, $\sigma_t = 3.7$ ns

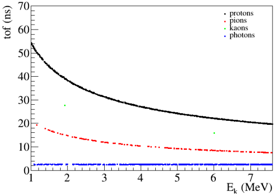

Dpmjet3 pp simulation
non elastic events, $\sigma_t = 0$

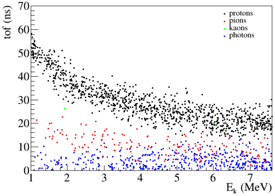

Dpmjet3 pp simulation
non elastic events, $\sigma_t = 3.7$ ns

- Here DPMJET3 set to decay π^0s

Pythia6, pp RHIC

Generated events: 1M, $E_{\mathrm{beam}} = 255$ GeV, w/ detector acceptance cut

PID	Particle	Entries
-321	K^-	6
-211	π^-	5697
-12	$\bar{\nu_e}$	2
-11	e^-	182
11	e^+	199
12	ν_e	1
13	μ^-	1
22	γ	32197
130	K_L^0	31
211	π^+	10339
321	K^+	129
2112	n	21
2212	p	97255

ProcessID	Process	Entries
1	$f_i \bar{f_j} \to \gamma^*/Z^0 \to F_K \bar{F_k}$	0
2	$f_i \bar{f_j} \to W^+ \to F_k \bar{F_l}$	0
10	$f_i f_j \to f_k f_l$	0
11	$q_i q_j \to q_i q_j$	15769
12	$q_i \bar{q}_i \to q_k \bar{q}_k$	14
13	$q_i \bar{q}_i \to gg$	31
14	$q_i \bar{q}_i \to g\gamma$	1
28	$q_i g \to q_i g$	8949
29	$q_i g \to q_i \gamma$	0
53	$gg \to q_k \bar{q}_k$	141
68	$gg \to gg$	8950
82	$gg \to Q_k \bar{Q}_k$	0
91	elastic scattering	88859
92	single diffraction ($AB \to XB$)	9791
93	single diffraction ($AB \to AX$)	8580
94	double diffraction	4974
95	low-p_T production	0
96	semihard QCD $2 \to 2$	0
114	$gg \to \gamma\gamma$	0
115	$gg \to g\gamma$	0

Pythia6, pp RHIC, TOF vs E_{kin} w/ PID

Generated events: 1M, $E_{\mathrm{beam}} = 255$ GeV, w/ detector acceptance cut

Process 1

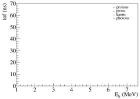

Process 2

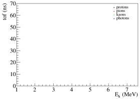

Process 10

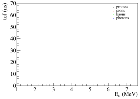

Process 11

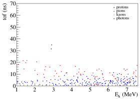

Process 12

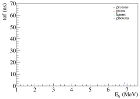

Process 13

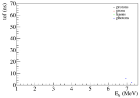

Process 14

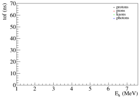

Process 28

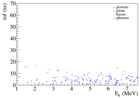

Process 29

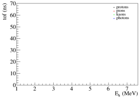

Process 53

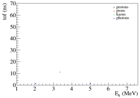

ProcessID	Process
1	$f_i \bar{f}_j \rightarrow \gamma^* / Z^0 \rightarrow F_K \bar{F}_k$
2	$f_i \bar{f}_j \rightarrow W^+ \rightarrow F_k \bar{F}_l$
10	$f_i f_j \rightarrow f_k f_l$
11	$q_i q_j \rightarrow q_i q_j$
12	$q_i \bar{q}_i \rightarrow q_k \bar{q}_k$
13	$q_i \bar{q}_i \rightarrow gg$
14	$q_i \bar{q}_i \rightarrow g\gamma$
28	$q_i g \rightarrow q_i g$
29	$q_i g \rightarrow q_i \gamma$
53	$gg \rightarrow q_k \bar{q}_k$

Pythia6, pp RHIC, TOF vs E_{kin} w/ PID

Generated events: 1M, $E_{\mathrm{beam}} = 255$ GeV, w/ detector acceptance cut

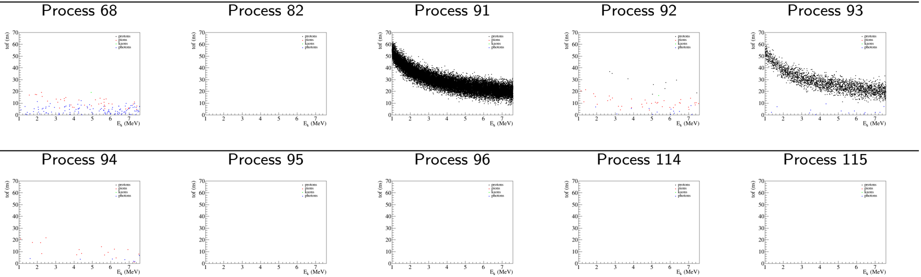

ProcessID	Process
68	$gg \to gg$
82	$gg \to Q_k \bar{Q}_k$
91	elastic scattering
92	single diffraction ($AB \to XB$)
93	single diffraction ($AB \to AX$)
94	double diffraction
95	low-p_T production
96	semihard QCD $2 \to 2$
114	$gg \to \gamma\gamma$
115	$gg \to g\gamma$

DPMJet-III, pp RHIC

Generated events: 1M, $E_{\mathrm{beam}} = 255$ GeV, w/ detector acceptance cut

PID	Particle	Entries
-321	K^-	18
-211	π^-	6236
-11	e^-	196
11	e^+	204
22	γ	35668
130	K_L^0	47
211	π^+	10628
310	K_S^0	48
321	K^+	124
2112	n	4
2212	p	89165

ProcessID	Entries
1	46624
2	85443
3	0
4	6
5	3067
6	5498
7	1700
8	0

DPMJET subprocesses in ep/eA

process1	Description
1	non-diffractive inelastic scattering
2	purely elastic scattering
3	quasi-elastic scattering
4	central diffraction (double-pomeron scattering)
5	single diffractive dissociation of particle 1
6	single diffractive dissociation of particle 2
7	double diffractive dissociattion
8	hard direct interactions

DPMJet-III, pp RHIC

Generated events: 1M, $E_{\mathrm{beam}} = 255$ GeV, w/ and w/o detector acceptance cut

WITHOUT acceptance cut

TOF vs E_{kin}
Non elast., w/ PID

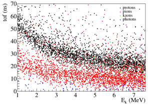

TOF vs E_{kin}
Non elast.

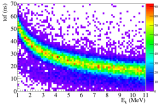

TOF vs E_{kin}
Protons

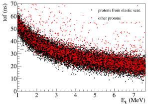

θ vs E_{kin}
w/ PID

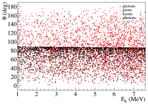

θ vs E_{kin}
Protons

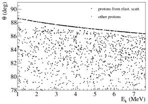

WITH acceptance cut

TOF vs E_{kin}
Non elast., w/ PID

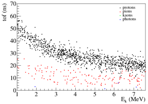

TOF vs E_{kin}
Non elast.

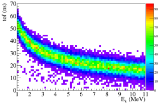

TOF vs E_{kin}
Protons

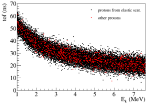

θ vs E_{kin}
w/ PID

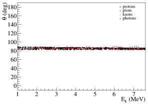

θ vs E_{kin}
Protons

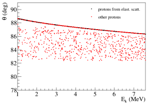

DPMJet-III, pp RHIC, TOF vs E_{kin}

Generated events: 1M, $E_{\mathrm{beam}} = 255$ GeV, w/ detector acceptance cut

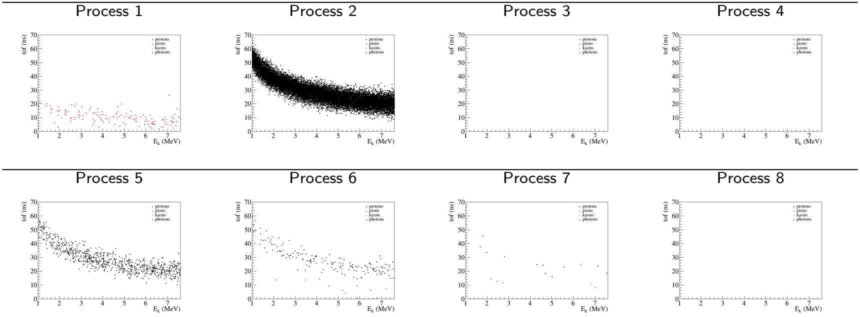

DPMJET subprocesses in ep/eA

process1	Description
1	non-diffractive inelastic scattering
2	purely elastic scattering
3	quasi-elastic scattering
4	central diffraction (double-pomeron scattering)
5	single diffractive dissociation of particle 1
6	single diffractive dissociation of particle 2
7	double diffractive dissociattion
8	hard direct interactions

DPMJet-III, pp RHIC, θ vs $E_{\rm kin}$ w/ PID

Generated events: 1M, $E_{\rm beam} = 255$ GeV, w/ detector acceptance cut

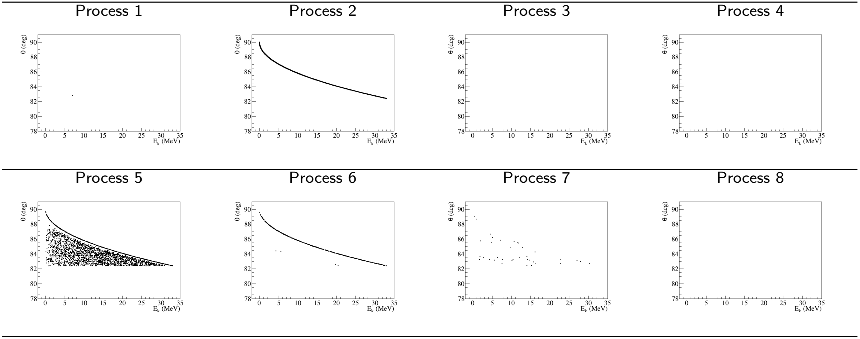

DPMJET subprocesses in ep/eA

process1	Description
1	non-diffractive inelastic scattering
2	purely elastic scattering
3	quasi-elastic scattering
4	central diffraction (double-pomeron scattering)
5	single diffractive dissociation of particle 1
6	single diffractive dissociation of particle 2
7	double diffractive dissociattion
8	hard direct interactions

DPMJet-III, pp RHIC, θ vs E w/ PID

Generated events: 1M, $E_{\mathrm{beam}} = 255$ GeV, w/o detector acceptance cut

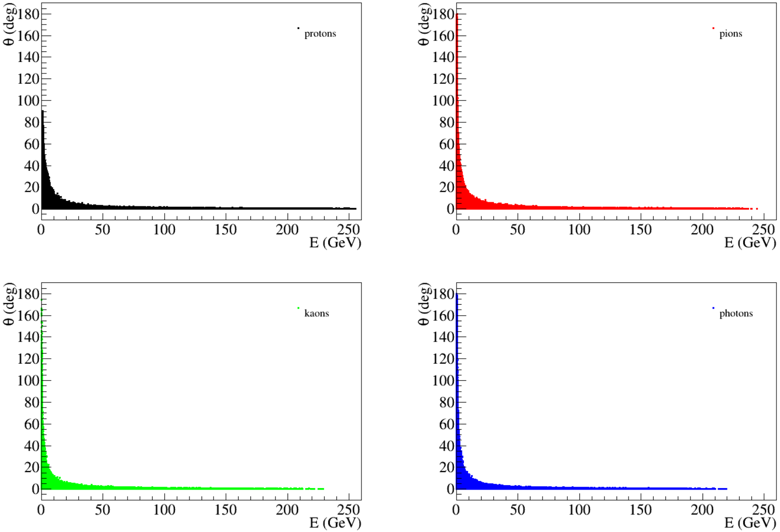

Summary and outlook

Done:

- Simulation of present polarimeters in DPMJet-III started
- Current H-Jet polarimeter data reasonably described by simulations of Pythia6 and DPMJet-III

To do:

- Simulate in DPMJet-III: dd, hh in RHIC ‘H-Jet’ polarimeter, pC and pAu in RHIC ‘Carbon’ polarimeters, pC and hC in AGS ‘Carbon’ polarimeters

BACKUP

Polarimetry at RHIC

- In contrast to lepton polarimetry, **hadron polarimetry doesn't use a physical process that can be calculated from first principles**
- Requirements: **precision** measurements, **polarization profile** and **lifetime** to know **polarization in collisions** in experiments
- A **two-tier measurement** is needed: one for the **absolute polarization** (with low statistical power), and one for **relative polarization** (with high statistical power)

- At RHIC, the absolute polarization is measured with the **H-Jet polarimeter**, and the relative polarization is measured by 4 **proton-carbon polarimeters**
- There are also **local polarimeters** at the experimental interaction regions, to define the spin direction and the degree of rotation in the experimental area

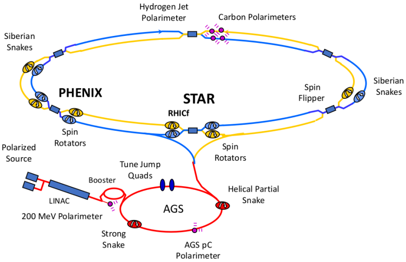

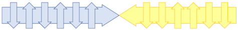

120 bunches (106 ns spacing)
10^{11} protons per bunch
Store $\sim$ 8 hours

Absolute Polarimeter: the H-Jet

- A **polarized proton jet, with known polarization** (measured with a Breit-Rabi polarimeter) is used as target for **elastic scattering in CNI region** by beam $\vec{p}$. Asymmetry: $\varepsilon = A_N P$.
- The analyzing power A_N doesn't have to be known and allows the **self-calibration** of the polarimeter
- **Left-right asymmetries** ε are extracted
- Beam polarization given by

$$P_{\text{beam}} = \frac{\varepsilon_{\text{beam}}}{A_N} = -\frac{\varepsilon_{\text{beam}}}{\varepsilon_{\text{target}}} P_{\text{target}}$$

- Silicon strips detect the recoil particles
- Pros: provides absolute values of polarization
- Cons: low statistics (because of diffuse target) limits the precision, doesn't allow online monitoring, nor measuring the polarization transverse and longitudinal profile, nor measuring the polarization lifetime, only per fill measurements

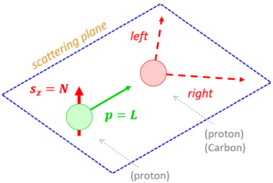

$$\varepsilon = \frac{N_L - N_R}{N_L + N_R}$$

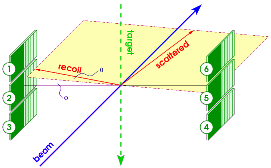

Fast and Precise Polarimeter: the pC Polarimeter

- **Non-polarized, ultra-thin carbon ribbon** ($w = 10$ μm), used as target for **elastic scattering in the CNI region** by beam $\vec{p}$
- Azimuthal asymmetries $\varepsilon(\phi)$ measured
- A_N from normalization to the H-Jet; dependence with energy agrees well with models
- Beam polarization: $P_b = \dfrac{\varepsilon(\phi)}{A_N \cdot \sin(\phi)}$
- Silicon strips detect the recoil particles, measurements of 20-30 s in target scan mode
- Pros: the high statistics allows precise measurements (**statistical precision 2-3%**), online monitoring, measurement of the **polarization transverse and longitudinal profile**, **polarization lifetime**, and fill by fill polarization
- Cons: stability of targets, calibration of Si detectors every year

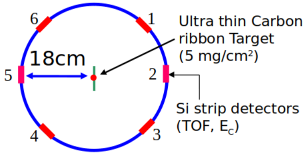

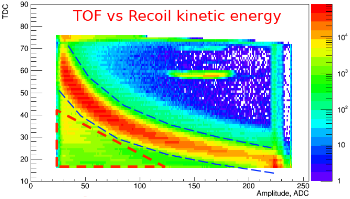

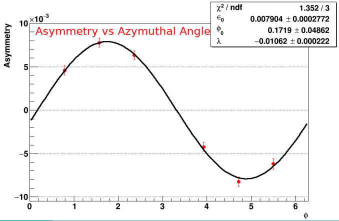

EIC Hadron Polarimetry

Requirements:

- Large polarization, long. and transv., flexible bunch polarization orientation
- Small uncertainty in polarization measurement: $\sim$1%
- Bunch polarization profile in x, y and z, polarization lifetime
- **Polarization per bunch** (2 detectors, not all bunches collide at a given IP)

Challenges:

- Short spacing between bunches
- Background to the signal events may contaminate preceeding bunch
- Luminosity measurement may depend on the polarization: $\sigma_{\text{Brems.}} = \sigma_0(1 + aP_eP_h)$
- **Pioneering light ion beam polarization measurements at high energies**

RHIC data:

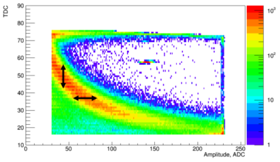

Bunch length

Detector resolution

120 bunches → 1320 bunches
106 ns → 8.9 ns

EIC (simulation):

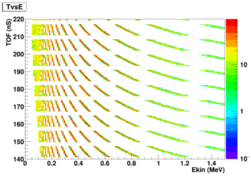

Polarized Proton Beams

- Problems: **background** to the elastic scattering events “banana” from triangular region in plot, **“prompts”** from the following bunch
- Ideas for improvements: second layer of silicon detectors can be installed in the polarimeters to **veto prompts** (to be tested in 2021 in pC and H-Jet polarimeters)
- **Other materials** could be used for more stable nuclear targets
- Silicon detectors and associated electronics (now: wave form digitizers) polarimeters can be upgraded to get **better timing resolution**

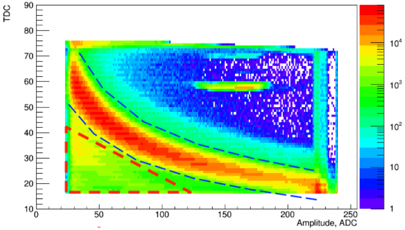

Background asymmetry, 10 measurements of RHIC pC polarimeters in 2017:

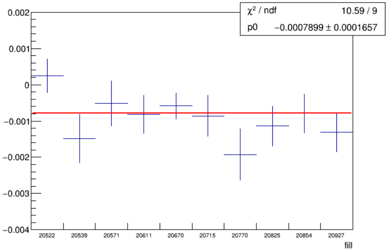

EIC parameter table

Table 3.3: eRHIC beam parameters for different center-of-mass energies $\sqrt{s}$, with strong hadron cooling. High divergence configuration.

Species	proton	electron	proton	electron	proton	electron	proton	electron	proton	electron
Energy [GeV]	275	18	275	10	100	10	100	5	41	5
CM energy [GeV]	140.7		104.9		63.2		44.7		28.6	
Bunch intensity [10^{10}]	20.5	6.2	6.9	17.2	6.9	17.2	4.7	17.2	2.6	13.3
No. of bunches	290		1160		1160		1160		1160	
Beam current [A]	0.74	0.227	1	2.5	1	2.5	0.68	2.5	0.38	1.93
RMS norm. emit., h/v [μm]	4.6/0.75	845/72	2.8/0.45	391/24	4.0/0.22	391/25	2.7/0.27	196/20	1.9/0.45	196/34
RMS emittance, h/v [nm]	16/2.6	24/2.0	9.6/1.5	20/1.2	37/2.1	20/1.3	25/2.6	20/2.0	44/10	20/3.5
β^*, h/v [cm]]	90/4.0	59/5.0	90/4.0	43/5.0	90/4.0	167/6.4	90/4.0	113/5.0	90/7.1	196/21.0
IP RMS beam size, h/v [μm]	119/10		93/7.8		183/9.1		150/10		198/27	
K_x	11.8		11.9		20.0		14.9		7.3	
RMS $\Delta\theta$, h/v [μrad]	132/253	202/202	103/195	215/156	203/227	109/143	167/253	133/202	220/380	101/129
BB parameter, h/v [10^{-3}]	3/2	100/100	14/7	73/100	10/9	75/57	15/10	100/66	15/9	53/42
RMS long. emittance [10^{-3}, eV·sec]	36		36		21		21		11	
RMS bunch length [cm]	6	0.9	6	2	7	2	7	2	7.5	2
RMS $\Delta p/p$ [10^{-4}]	6.8	10.9	6.8	5.8	9.7	5.8	9.7	6.8	10.3	6.8
Max. space charge	0.006	neglig.	0.003	neglig.	0.028	neglig.	0.019	neglig.	0.05	neglig.
Piwinski angle [rad]	5.6	0.8	7.1	2.4	4.2	1.2	5.1	1.5	4.2	1.1
Long. IBS time [h]	2.1		3.4		2		2.6		3.8	
Transv. IBS time [h]	2		2		2.3/2.4		2/4.8		3.4/2.1	
Hourglass factor H	0.86		0.86		0.85		0.83		0.93	
Luminosity [10^{33}cm^{-2}sec^{-1}]	1.65		10.05		4.35		3.16		0.44	

Interaction of photons with matter (carbon and lead)

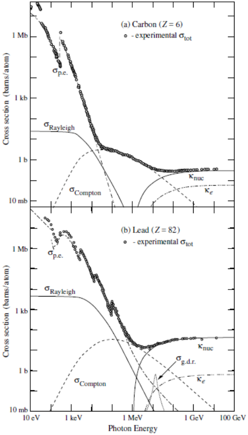

Figure 33.15: Photon total cross sections as a function of energy in carbon and lead, showing the contributions of different processes [50]:

$\sigma_{p.e.}$ = Atomic photoelectric effect (electron ejection, photon absorption)
$\sigma_{Rayleigh}$ = Rayleigh (coherent) scattering–atom neither ionized nor excited
$\sigma_{Compton}$ = Incoherent scattering (Compton scattering off an electron)
κ_{nuc} = Pair production, nuclear field
κ_e = Pair production, electron field
$\sigma_{g.d.r.}$ = Photonuclear interactions, most notably the Giant Dipole Resonance [51]. In these interactions, the target nucleus is usually broken up.

Original figures through the courtesy of John H. Hubbell (NIST).